TRABAJO DE FIN DE GRADO

Grado en Biomedicina

Design and Characterization of an Optogenetic Tool to Investigate the Neurotoxicity of *Escherichia coli* Amyloid CsgA Fimbriae in *Caenorhabditis elegans.*

Autor: Lucía Rodriguez Heine

Villaviciosa de Odón,

15/05/2025

Information about the center

The CNB – CSIC is one of the most important research institutes in Spain in the field of biotechnology and biomedicine. It was founded in 1992 as part of the Spanish National Research Council (CSIC), whose main objective is to promote scientific research of excellence with a multidisciplinary approach. This approach aligns with the World Health Organization's vision that today's research requires increased collaboration between institutions, moving away from compartmentalized research. The CNB focuses on four main research areas: infectious diseases, inflammation and cancer, sustainability of food production, and bioremediation. To support these goals, the CNB is structured into six departments: Systems Biology, Immunology and Oncology, Molecular Genetics of Plants, Cell and Molecular Biology, and Macromolecular Structure.

There are four key words that summarize the CNB's institutional and scientific strategy: training, leadership, collaboration, and knowledge transfer. Regarding training, the CNB prioritizes the education of researchers through seminars and courses. Moreover, it is a center where many students, like myself, have the opportunity to begin their research careers. As for collaboration, over the years, the CNB has participated in international consortia and collaborated with prestigious universities. Additionally, the CNB emphasizes the transfer of high-quality knowledge, as many of its members and research groups have published papers in high-impact journals.

Today, the CNB is considered a leading biotechnology center in both Spain and Europe. Every four years, the CNB must submit a strategic plan to the CSIC presidency for approval. For the 2022–2026 period, one of the main objectives is the renewal of the Severo Ochoa Center of Excellence Accreditation. Through this accreditation, the CNB will be able to continue pursuing its goals of leadership, training, collaboration, and knowledge transfer, by following the strategies outlined below:

1. Consolidating and expanding national and international leadership and collaborations.
2. Strengthening the bioimaging initiative to improve quantification through image analysis.
3. Promoting internal synergy between CNB research groups.
4. Continuing with the transfer of technologies (patents).

Abstract

Previous studies on bacterial amyloids (like curli from *E.*coli) have shown that some have the capacity to cross – seed with human neural proteins (Friedland et al., 2020) and induce cell toxicity (Molina-García et al., 2017, Revilla García, 2019). Moreover, it has been seen that curli has the ability to reach neurons in *Caenorhabditis elegans* (C. elegans) model (C. Wang et al., 2021).Nevertheless, it has not been studied if these functional bacterial amyloids (FUBAs) have the capacity to induce neurotoxicity per se.

In this study we designed and characterized an optogenetic fusion protein, CsgA-CRY-mCherry based on a tool already developed for the Aß peptide (Lim et al., 2020) to investigate the neurotoxic potential of curli major subunit CsgA in *C. elegans.* This animal model will permit us to investigate the neurotoxic pathways as it has its entire connectome mapped out. The construct enables light dependent oligomerization of CsgA *in vivo* allowing the control of its aggregation. Moreover, we also designed an Aß-CRY-mCherry plasmid as a possitive control for neurotoxicity.

We show through Congo Red assays in *E. coli* mutants a potential light-induced amyloid formation of the CsgA-CRY-mCherry plasmid, yet, protein expression was not able to be detected by western blot due to technical limitations.

Introduction

Over the decades, there have been studies in animals that have shown the importance of the gut microbiome in regulating the central nervous system (CNS). The bidirectional comunication of the microbiota-gut-axis has been deeply studied and shows growing evidence of how the gut microbiota plays a critical role in the progression and severity of the symptoms of neurodegenerative diseases such as Parkinson´s or Alzheimer´s disease. disease (Cryan et al., 2020) (C. Wang et al., 2021). There are studies that show how alterations in the composition of gut microbiome are linked to Parkinson´s disease (Unger et al., 2016), Multiple Sclerosis (Berer et al., 2011), Alzheimer's disease (Fujii et al., 2019) and schizophrenia (Zheng et al., 2019).Nevertheless, the molecular mechanism by which this correlation occurs remains yet unclear. The question that arises is whether the microbiota´s proteins or metabolites can act directly on the host neurons and therefore further aggravate the neurodegenerative process (Friedland et al., 2020).

All these diseases share a common characteristic which is the accumulation of neural proteins that have a prion – like feature. These aggregated proteins have the capacity to induce the aggregation of misfolded proteins and move from one region of the body to another, yet the mechanism by which the aggregation is initiated is still unknown. Prusiner suggested that it is a result of a stochastic misfolding of the prion–like protein (Prusiner, 2012).

Among neurodegenerative diseases, Alzheimer´s disease is one of the most common type of dementia around the world, estimated 60 – 80% of all the cases of dementia worldwide. Around 1% of the cases inherit the disease while the rest manifest the pathology in a sporadic manner. Nevertheless, the clinical and molecular picture of the disease is similar for both cases. On a molecular basis, Alzheimer´s disease presents an aberrant aggregation of proteins, aberrant metabolism, alterations in the homeostasis of proteins, cytoskeleton abnormalities and disfunction in the neural networks. The extracellular aggregation of the Aß is the most studied molecular marker of the disease. The Ab42 isoform, which is the most pathogenic, is produced by the amyloidogenic pathway through the cleavage of the amyloid precursor protein by the ß-secretase. It is a small peptide consisting of 37-43 amino acids and has the capacity to form extracellular insoluble fibrils (Orobets & Karamyshev, 2023). The structure of the fibrils usually consists of a cross β-sheet. The formation of insoluble fibers typically consists of a nucleation phase followed by an elongation phase.

Functional bacterial amyloid proteins (FuBAs), originally discovered by Chapmann and colleagues, are proteins that in bacteria help the organisms stick together and promotes bacterial communities (X. Wang et al., 2008). These amyloids have been found in both gram positive and negative bacteria (Taylor & Matthews, 2015). The human body harbors trillions of microbes, primarily located in the gut, many of which are capable of producing functional bacterial amyloids (FuBAs) (Friedland & Chapman, 2017) . Out of all the bacterial amyloid proteins, the extracellular fiber called curli made by *Escherichia coli* has been the most studied one (Chen et al., 2016).

Curli is classified as a functional amyloid – a protein that assembles into highly ordered β-sheet-rich fibers and are beneficial to bacteria. This cellular adhesin is known to mediate host–cell adhesion, biofilm formation and immune system activation (Perov et al., 2019). Curli formation in *E.coli* and other Enterobacteriaceae is controlled by a specialized system called the curli biogenesis system (Taylor & Matthews, 2015) as shown in **figure 1**. This system involves genes encoded by two distinct operons, *csgBA* and *csgDEF.* and at least six proteins (Barnhart & Chapman, 2006). The *csgBA* operon codifies for the major structural subunit which is csgA and csgB which is the nucleator protein (Hammar et al., 1995). Polimerization of the mayor subunit, csgA, is nucleation dependent. In the absence of csgB, csgA is secreted to the extracellular compartment in a soluble form (Nenninger et al., 2009). Specifically, there are four internally conserved Gln and Asn residues in csgA which are necessary for csgB-mediated nucleation (X. Wang & Chapman, 2008). When these four residues are mutated, the protein had no abilithy to respond to nucleation by csgB. Structural results obtained from X-ray diffraction show that csgA possesses a cross-ß-architecture which is similar to the human pathological amyloids. It is interesting to note that in its sequence, csgA has a short oligopeptide repeat which is similar to prion protein repeats (Cherny et al., 2005). csgA fibers bind to Congo Red which is a commonly used dye for amyloid detection (Frid et al., 2007)

csgDEFG encodes for other four proteins needed for curli assembly. csgD is a protein whose C-terminal region shares homology with DNA-binding motifs. Mutations in the csgD gene have been shown to suppress transcription of the *csgBA* operon, suggesting its function as a transcription factor (Hammar et al., 1995). csgG is found in the bacterial outer membrane (as shown in **figure 1**)and it is a key component of the curli system. Its ß-barrel structure forms a secretion channel that facilitates translocation of the curli subunits to the extracellular space (Taylor & Matthews, 2015). There is a 22- aminoacids sequence in csgA that is responsible of directing the protein towards the csgG secretion apparatus (Robinson et al., 2006). In relation

to the csgF protein, in a csgF mutant, it has been seen that csgA is largely secreted away from the cell in a soluble state (Chapman et al., 2002). Moreover, it has been seen through an interbacterial complementation that this protein is necessary in the nucleation step and that it interacts with csgB to facilitate its nucleator function (Nenninger et al., 2009). All this indicates that csgF acts as an anchor for csgA near the bacterial surface and stabilizes the nucleation process by interacting with csgB. Moreover, another key protein in this tightly regulated process of curli formation is csgC. It has been seen that this protein is responsible for inhibiting csgA fibrillation (Evans et al., 2015) and therefore preventing premature amyloid formation which results toxic to the bacteria.

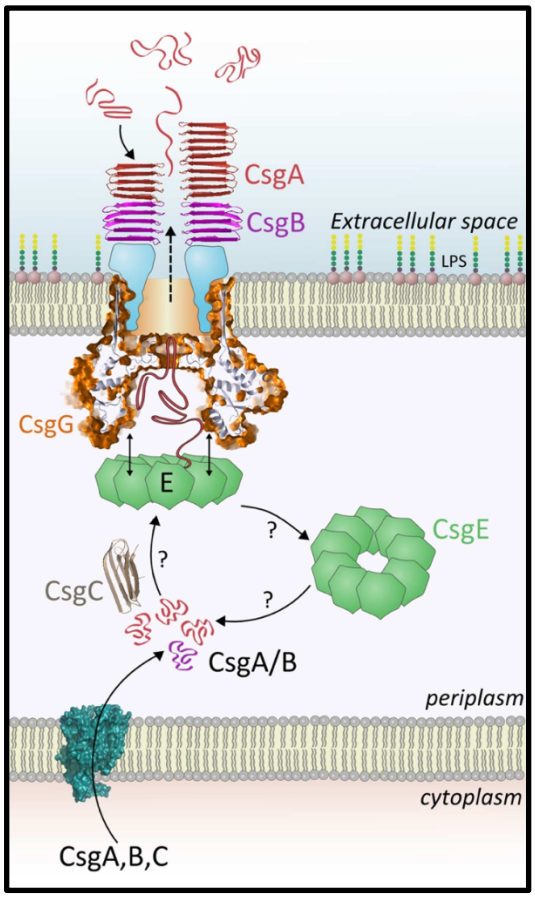

Figure 1. Schematic representation of curli biogenesis taken from Taylor & Matthews, 2015

While curli plays an important physiological role in bacteria, several studies have highlighted its pathogenic role in humans. For example, research has shown that curli has the capacity to activate several proinflammatory innate immune receptors (Tursi & Tükel, 2018), with the promotion of human autoimmune disorders (Gallo et al., 2015) and prevalence of Parkinson´s disease (Chen et al., 2016). Notably a study conducted by Wang et al in 2021

demonstrated the capacity of curli to reach neurons and induce the aggregation of α -synuclein (C. Wang et al., 2021)

Previous studies on bacterial amyloids have shown that some of these amyloids have the capacity to cross-seed with human neural proteins (Friedland et al., 2020). Cross-seeding refers to the ability of one misfolded molecule to induce the misfolding of another molecule. Once the initial seeds are formed, the amyloid fibrils have the capacity to grow *in vivo* by recruiting monomeric units. Thus, the presence of bacterial amyloids may reduce the lag time in the spontaneous and nucleation-dependent generation of human amyloid fibrils (O'Nuallain et al., 2004). Nevertheless, it has also been described that bacterial amyloids on their own can induce cytotoxicity through mechanisms similar to those observed for human pathological amyloids. A well-described pathway involves the targeting of the plasma membrane and the formation of pore-like structures, ultimately leading to cell death (Molina-García et al., 2017), Revilla García, 2019). Given the finding that curli, and maybe other bacterial amyloids, have the capacity to reach the brain in a *C. elegans* model and have been described to induce cell toxicity, it becomes interesting to investigate the neurotoxic effects per se of bacterial amyloids.

C. elegans has evolved as an outstanding animal model for biological research due to its simplicity, transparence and that it can be easily maintained. They are cultured in agar plates containing Nematode Growth Medium (NGM) and they feed on bacteria. Usually they are fed with the strain of *E. coli* OP50. Other benefits include their short lifecycle and that they are easy to manipulate genetically. These nematodes can be hermaphrodites – that self-fertilize – or males. Thus, if hermaphrodites are mutated, this mutation will be present in the next generations due to self-fertilization (Torres et al., 2025).

In the context of neurodegeneration research, *C. elegans* offers several unique advantages. Its well-studied, described and compact nervous system is particularly beneficial (Torres et al., 2025). The fact that it has exactly 300 neurons reduces the complexity and facilitates the analysis (Cook et al., 2019). Additionally, the entire connectome of the nervous system of *C. elegans* is mapped out. This gives us precise understanding of the neural circuits in *C. elegans* and allow us to perform functional studies and model neurodegenerative diseases. Moreover, almost 42% of the protein-coding genes in *C. elegans* have identifiable human orthologs (Kim et al., 2018). This highly gene conservation is of extreme value for the investigation of molecular pathways and cellular mechanisms underlying neurodegenerative disorders.

Given the evidence that bacterial amyloids can reach the brain in *C. elegans* animal model and can potentially induce neurodegeneration, it becomes crucial to understand which are the underlying neurotoxic mechanisms. In this work, we aim to characterize the aggregation behavior and neurotoxic potential of the curli subunit csgA *in vivo* using *C. elegans* as a model organism. So, to directly visualize the aggregative effects of bacterial amyloids and control aggregation dynamics in neurons, we engineered a neural expression construct that contains the amyloidogenic protein csgA, a modified version of the light sensitive CRY2 domain from *Arabidopsis thaliana* (CRY2PHR) and the red fluorescent protein mCherry. This protein fusion will therefore have the ability to oligomerize under blue light, and thus, we will be able to characterize the neurotoxic effect of csgA oligomerization *in vivo*.

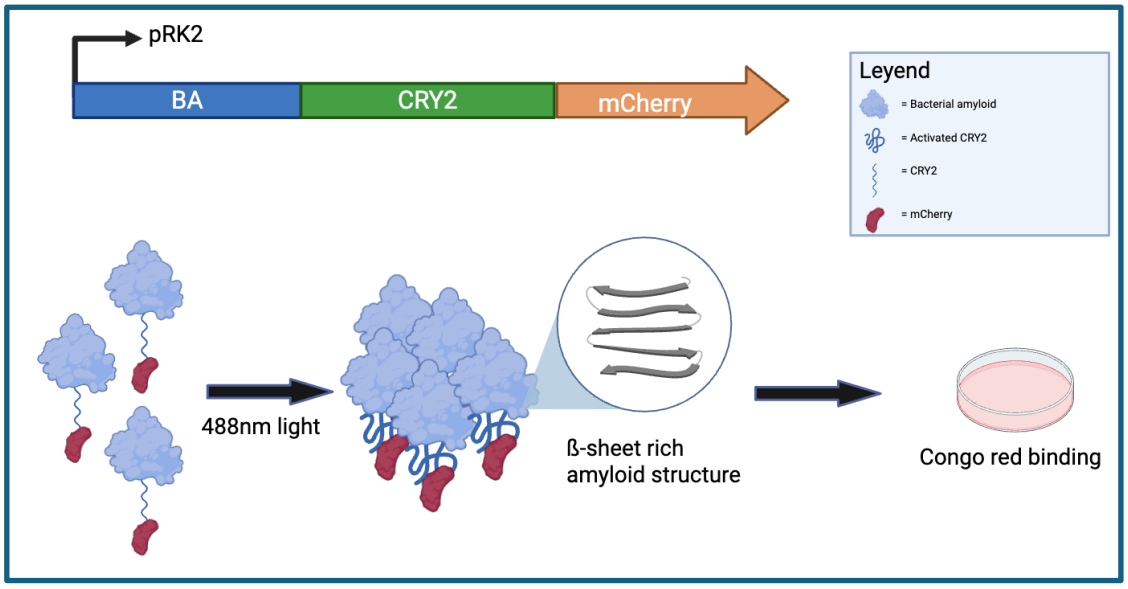

Figure 2. Optogenetic tool upon blue light exposure. Image shows the effect of blue light induction on the cryptochrome 2 and how amyloid fibrils can then be assessed by using Congo Red binding.

Objetives

1. **Development and characterization of the optogenetic tool.**

In order to assess the *in vivo* of the oligomerization of bacterial amyloids we used an optogenetic tool which was previously developed in *C. elegans* to study the effects of soluble *vs*. oligomeric Aß peptide (Lim et al., 2020). This system allows us spatiotemporal control of amyloid oligomerization through light stimulation. This system consists of three components: the amyloidogenic protein, the light sensitive CRY2 domain (*Arabidopsis thaliana*

cryptochrome 2 (CRY2) protein which oligomerizes quickly and reversibly in the presence of blue light at 488nm) and a variant of the red fluorescent protein mCherry.

In the reference study (Lim et al., 2020), the fusion protein was expressed under a heat shock promotor to minimize toxicity, which can occur with constitutive promotors. In our case, we opted for a multi copy neural promotor (Rab3) to achieve stable neuron-specific expression.

2. Characterization of the amyloidogenic capacity of the CsgA-CRY-mCherry fusion protein.

To evaluate the light – dependent amyloidogenic behavior of the CsgA-CRY-mCherry protein fusion, we assessed its aggregation dynamics under light and dark conditions using Congo Red staining, a classical method for detecting amyloid structures.

E. coli cultures were grown in agar plates containing IPTG and Congo Red staining and were grown in light / dark conditions in order to assess differences in amyloid aggregation.

3. Study the toxicity of the Aß-CRY-mCherry protein fusion in *C. elegans.*

A lifespan assay was performed in order to see the toxicity of the Aß-CRY-mCherry in *C. elegans.* The lifespan of transgenic nematodes was compared to the lifespan of non – transgenic nematodes. Moreover, I also compared the lifespan between nematodes exposed to blue light and those under dark conditions.

Theoretical framework

There is growing evidence about a bidirectional communication between the gut microbiota and the central nervous system. It has been seen that the gut microbiome can have implications in neurodegenerative diseases for example Alzheimer´s Disease or Parkinson's disease. For example, gut microbiome dysbiosis has been seen in patients that have Parkinson´s disease (Unger et al., 2016). The question that arises next is how the microbiome is able to modulate these diseases. There are several pathways proposed; the gut-brain axis, the secretion of toxic proteins, the modulation of the production of short chained fatty acids, tryptophan, branch-chained amino acids, modulating the inmune system, a cross-seeding with human pathogenic amyloids and more (Intili et al., 2023) (Loh et al., 2024).

As there is a rise in the global prevalence of neurodegenerative diseases and the fact that there are not perfect treatments for them, it becomes important the need to discover new therapeutic agents to be able to tackle these diseases.

Methods

1. DNA manipulation.

1.1 Preparation of competent cells and transformation.

1.1.1 Chemically competent cells.

Chemically competent *E. coli* DH5α or BW25113 (Δ*csgA*) and BW25113 (Δ*csgB*) cells were prepared by inoculating 5mL of LB either without antibiotic (for DH5α cellls) or supplemented with 50µg/mL of kanamycin(to select for the deletion mutant phenotype) and left incubating overnight at 37 °C. The next day, 100µL of the overnight culture were added to 10mL of LB containing 10mM SO_4Mg and 0.2% glucose. The culture was then grown to an OD_{600} of 0.3 – 0.4, divided into 2mL aliquots', centrifuged for 2 minutes at 12000 rpm at room temperature (RT) and resuspended in 100µL of ice-cold $CaCl_2$ 0.1M. Cells were incubated on ice 1h prior to transformation or mixed with sterile glycerol to a final concentration of 10 % for storage at -80°C.

1.1.2 Competent cell transformation.

1 µL of intact plasmid DNA or 20 µL of a Gibson assembly reaction was added to an aliquot of competent cells and incubated on ice for 30 minutes, followed by a heat shock at 42°C for 2 minutes. The tubes were returned to ice for another 10 minutes, then 900 µL of LB was added, and the mixture incubated at 37°C with shaking for 1 hour. This was then seeded in LB agar plates supplemented with the appropriate antibiotic.

1.2 Molecular cloning.

1.2.1 Molecular cloning *in silico.*

Plasmids were designed using the ApE (A plasmid Editor) software. T express CsgA in *C. elegans*, the protein -fused to the *Arabidopsis* thaliana cryptochrome 2 (CRY2) protein which oligomerizes quickly and reversibly in the presence of blue light at 488 nm (Hsien et al., 2020) and a variant of the red fluorescent protein mCherry- was cloned under the neural promotor *prab3* in a pD9575 plasmid (pBR322 derivative). For bacterial expression in *E.coli*, fusion genes were cloned into the low-copy-number plasmid pRK2.

1.2.2 Plasmid DNA extraction.

To extract plasmid DNA, O/N cultures were processed using the NZYminiprep (ZYtech) kit and following the manufacturer´s instructions.

1.2.3 Generation of vectors for transgenic *C. elegans.*

To generate the pRab3-Abeta-CRY-mCherry plasmid, CRY-mCherry fragment was PCR-amplified from a donor plasmid pDONOR-CRY-mCherry. The vector backbone was obtained by amplifying the pRab3-Abeta fragment from the pRab3-Abeta-NV1 plasmid. Gibson Assembly (**figure 3a**) was used to ligate the fragments

For the pRab3-CsgA-Abeta-CRY-mCherry plasmid, the *CsgA* (coding for the bacterial amyloid protein curli) was amplified from pRab3-CsgA-RFP and inserted into the vector pRab3-CRY-mCherry via Gibson Assembly. This vector was obtained amplifying the plasmid pRab3-Abeta-CRY-mCherry and without the Aß sequence.

The Gibson assembly reaction is a technique used to join two or more DNA fragments that have overlapping ends into a continuous DNA strand. To perform the reaction, the vector and insert (previously digested with Dpn1 and purified) are mixed in a 1:2 ratio, with each at a concentration of 100ng/µL, in a Gibson Assembly master mix. The mixture is then placed in a thermocycler for 1 hour at 50ºC .

1.2.4 Generation of expression vectors for *E. coli*.

For expression in *E. coli* , the CRY – mCherry fusion protein was PCR-amplified from the pRab3-CsgA-CRY-mCherry and cloned into pRK2-CsgA using Gibson Assembly, resulting in the following construct pRK2-CsgA-CRY-mCherry. The vector backbone was obtained amplifying the plasmid pRK2-CsgA-NV1 (previously generated in the lab), excluding the NV1 sequence. The primers used to design all the constructs of this study are listed in the Table 1 appendix.

The pRK2 vector (as shown in **figure 3c**) is inducible by IPTG as it is under the control of a *Ptac* promoter.

1.2.5 Construct verification.

Colony PCR was performed after transformation to identify colonies containing the correct assembly. PCR products were analyzed by agarose gel electrophoresis. Plasmid DNA was extracted from positive colonies and sent for Sanger sequencing to confirm the correct sequence of the insert with Eurofins company.

2. Characterization of optogenetic tool.

2.1 Congo Red assay for detection of amyloid aggregates.

In order to assess how the optogenetic tool behaved under light/dark conditions, *E.coli* BW25113 Δ*CsgA* + CsgA-CRY-mCherry, Δ*CsgB* + CsgA-CRY-mCherry, Δ*CsgB*, Δ*CsgA* and *E. coli* BW25113 wild type (wt) were grown in Congo Red agar plates for 48 hours under light or dark conditions at 25 ºC.

To prepare the Congo Red YESCAagar plates, the following components were added to a 2 L container. 1 g of yeast extract, 10 g of casamino acids, 10 mg/L of Coomassie Blue Stain and 20 g of agar. The mixture was then autoclaved for sterilization. After autoclaving, Congo Red was added at a concentration of 0.05 mg/mL, IPTG to induce the expression of CsgA-CRY-mCherry at 0.05 mM and the appropriate antibiotics. Two types of plates were prepared: one that contained kanamycin 50 µg/mL and ampicillin 50 µg/mL and another only with kanamycin. This is because the Δ*csgB* and Δ*csgA* mutants are generated with a kanamicyn resistance cassete and the pRK2-CsgA-CRY-mCherry plasmid the ampicilin resistance gene.

2.2 Protein induction and characterization by Coomassie Blue staining and western blotting.

To characterize the pRK2-CsgA-CRY-mCherry plasmid, protein expression was induced using IPTG. *E .coli* BW25113 Δ*csgA* (Baba et al., 2006) cells transformed with the pRK2-CsgA-CRY-mCherry plasmid were inoculated into 5 mL of LB supplemented with 100 µg/mL of ampicillin and 50 µg/mL of kanamycin and incubated overnight at 37 °C. The following day, the OD_{600} of the culture was measured and cells were diluted in 20 mL of fresh LB medium supplemented with the same antibiotics to an OD_{600} of 0.05. The culture was grown at 37 °C until it reached an OD_{600} of 0.3 – 0.4.

At this point, two 1 mL aliquots were taken: one was in order to fix so to then be able to visualize the protein through optical microscopy and the other was frozen for later analysis by western blot assay. The remaining culture was split into two equal volumes; IPTG was added to one half to a final concentration of 0.05 mM, while the other served as a non-induced control. The cultures were incubated at 37 °C and samples were collected at 1 h and 3 h post-induction. For each time point, the OD_{600} was recorded and 1 mL samples were collected for fixation and freezing, respectively.

2.2.1 Sample fixation for fluorescence microscopy

Collected samples were centrifuged, and the resulting pellets were washed three times with 500µL of 1x PBS. After the final wash, the supernatant was discarded, and the pellet was resuspended in 100 µL of a PFA/DAPI solution (100:1). The samples were then incubated for 30 minutes at room temperature in the dark. Following fixation, cells were washed twice with 200 µL of 1X PBS and finally resuspended in 100 µL of 1X PBS for storing at 4 °C.

For following fixation, 15 µL of the sample were placed onto a glass slide and then covered with polylysine. After drying, the samples were mounted using Vectashield mounting medium (Vector Laboratories)

2.2.2 Coomassie Blue stained SDS-PAGE

In order to verify the presence of the recombinant construct in *E. coli* after IPTG induction, a 10-12% SDS-PAGE gel was run followed by Coomassie Blue staining. Each well of the gel was loaded with bacterial sample adjusted to an OD_{600} of 1 resuspended in 50 µL of 5X Laemmli protein buffer. 25 µL of each samples were loaded into each well.

2.2.3 Western blot analysis

After completing SDS-PAGE, proteins were transferred using a semi-dry transfer system into a PVDF membrane (10 V, 2h). The membrane was blocked overnight at 4 °C in 5% non–fat dry milk prepared in TTBS (TBS 1X with 0.05% of Tween 20). The membrane was subsequently incubated with the primary antibody (Anti-csgA) diluted 1:1000 in 3mL of blocking buffer for 2 hours at room temperature. After incubation, the membrane was washed three times with TTBS (3 x 20 min at room temperature with gentle agitation). The membrane was then incubated with the secondary antibody diluted (Anti-Rabbit) 1:10 000 in 10mL of blocking buffer for 1 hour at room temperature followed by three additional washing steps in TTBS. Protein detection was performed using an enhanced chemiluminescence (ECL) substrate (and signal acquisition was conducted using a biorad digital imaging system (Bio-Rad laboratories) using a 1-minute exposure time.

4 Generation of transgenic *C.elegans* and expression of optogenetic transgenes

4.1 *C. elegans* growth conditions and maintenance

Caenorhabditis elegans strains were maintained on Nematode Growth Medium (NGM) agar plates that were seeded with *Escherichia coli* (OP50) as their food source (Taylor & Matthews, 2015). The NGM plates were prepared by autoclaving a mixture of 3 g NaCl, 2.5 g

peptone, and 17 g agar in 975 mL of distilled water. After autoclaving, 1mL of 1 M $CaCl_2$, 1mL of 1M $MgSO_4$, 25 mL of potassium phosphate buffer and 1 mL of 5mg/mL cholesterol were added. 12 mL of the mix was poured into plates and allowed to solidify before being seeded with 200 µL of overnight *E.coli* OP50 culture.

Worms were cultured in a 20 °C incubator. For routine maintenance, adult worms were transferred to freshly seeded NGM plates every 2-3 days to avoid overcrowding and starvation. For long term storage, the worms were suspended in a freezing buffer (40mL 5M NaCl, 100mL 1M KPO4, pH 6; 600mL glycerol, H_2O up to 2L) mixed 1:1 ratio with M9 buffer and stored in cryovials at -80 °C.

4.2 Generation of transgenic *C.elegans*

The process of generating transgenic *C. elegans* was performed by Laura Molina García (my supervisor and the principal investigator of the laboratory). This technique involves the injection of a mix containing CsgA-CRY-mCherry and another containing Aß-CRY-mCherry into the gonads of young adult hermaphrodite worms using a microneedle under a microscope. The injection mix contained DNA marker to identify the transgenic nematodes, the DNA plasmid containing the amyloidogenic protein and DNA crowder. The total DNA concentration in the mix was adjusted to 100ng/µL

4.3 Western blotting for validating protein expression in *C.elegans*

50 L4 hermaphrodites nematodes were manually picked and resuspended in a 50 µL Laemmli loading buffer. This mixture was then loaded into a SDS-PAGE gel. One gel was used for Coomassie Blue staining and the other was used for western blot. The primary antibody used was Anti-mCherry at a concentration of 1:1000 in order to identify the presence of the pRab3-Aß-CRY-mCherry construct. The secondary antibody was Anti-Rabitt at a concentration of 1:10000.

Results

1. Plasmids developed for bacterial and neural expression in *C. elegans* of the amyloid protein CsgA.

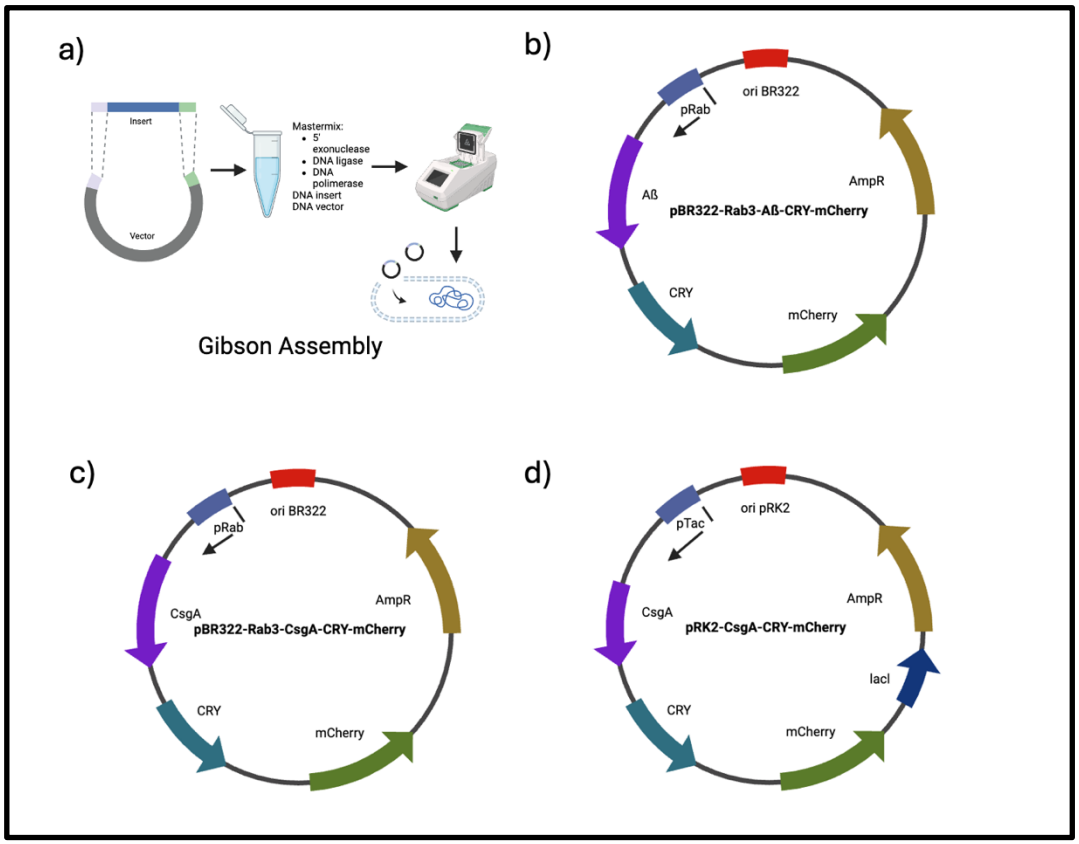

Figure 3. a) Gibson Assembly reaction, b, c, d) plasmids generated for evaluation of bacterial and neural expression in *C. elegans*.

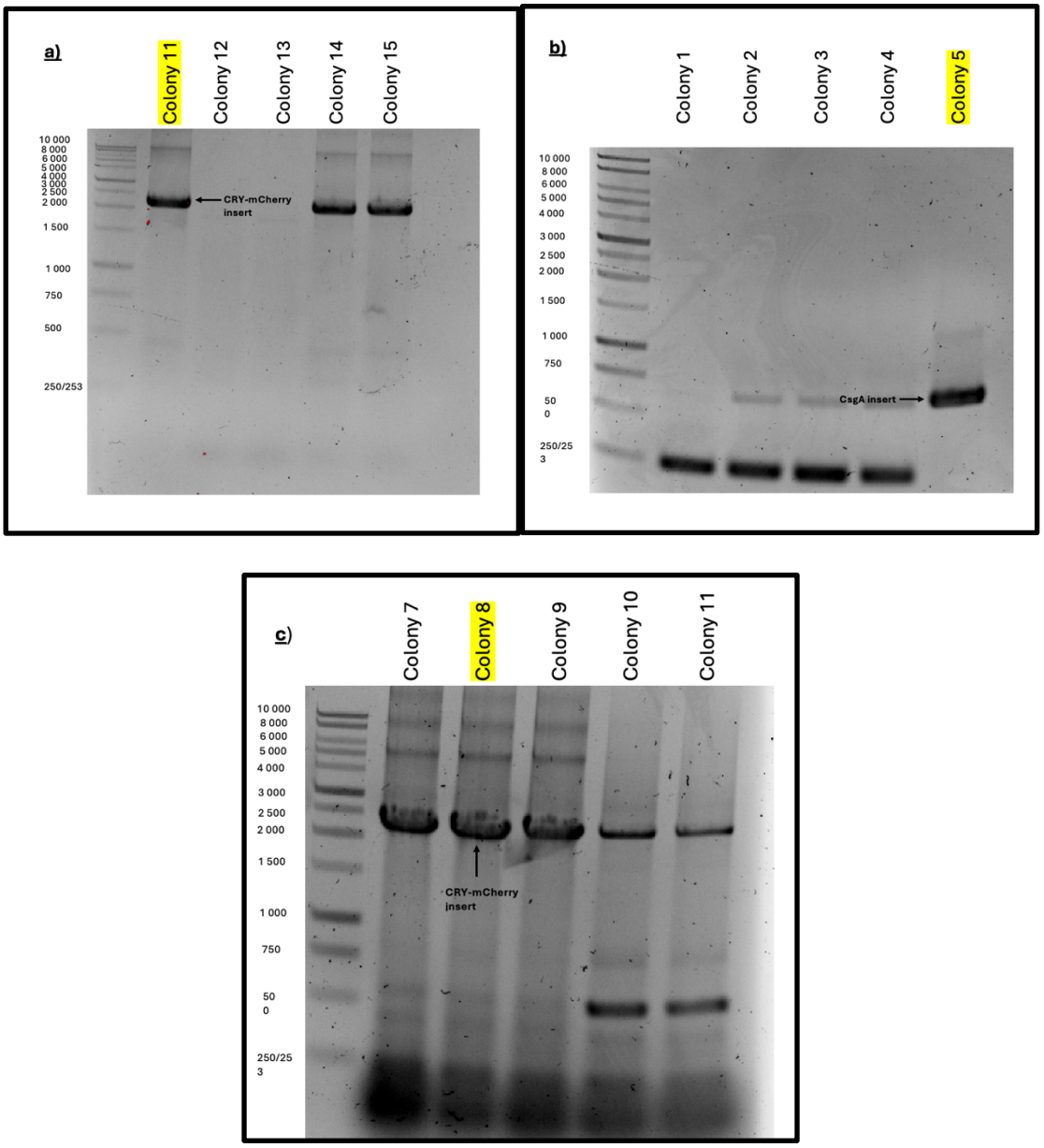

Figure 4; Positive clones identificated in transformed *E.coli* DH5-α. Pannel a) pRab3-Aß-CRY-mCherry b) pRab3-CsgA-CRY-mCherry c)pRK2-CsgA-CRY-mCherry

Three plasmids were created so to assess the aggregative and neurotoxic effects of CsgA subunit of the curli protein. These plasmids were generated through Gibson Assembly reaction. Procedure shown in **figure 3a).** The first plasmid generated was pRab3-Aß-CRY-mCherry through the amplification of the vector pRab3-Aß from the pRab3-Aß-NV2 plasmid and the amplification of the insert CRY-mCherry from the plasmid pDONOR-CRY-mCherry. In **figure 4a)** it can be seen presence of the insert CRY-mCherry of 2249pb in colonies 11, 14 and 15. Colony 11 was chosen for further sequencing so to verify that the plasmid had ensembled

correctly. This plasmid was created under the neural promotor Rab3 in order to have a positive control of aggregation for transgenic *C .elegans.*

The second plasmid generated was pRab3-CsgA-CRY-mCherry through the amplification of the vector pRab3-CRY-mCherry from the pRab3-Aß-CRY-mCherry plasmid and the amplification of the insert CsgA from the Rab3-CsgA-RFP plasmid. In **figure 4b)** it can be seen the presence of the insert CsgA of 610pb in colony 5 and a lighter band in colonies 2, 3 and 4. Yet, colony 5 was chosen for further sequencing to verify if the fragment was correct.

The third plasmid generated was pRK2-CsgA-CRY-mCherry through the amplification of the vector pRK2-CsgA from the pRK2-CsgA-NV1 plasmid and the amplification of the insert CRY-mCherry from the pRab3-CsgA-CRY-mCherry plasmid. In **figure 4c)** it can be seen the presence of the CRY-mCherry insert of 2249 pb in colonies 7, 8 and 9. Colonies 10 and 11 also had a band at that same weight but also an inespecific band at a lower weight. That is why colony 8 was chosen for further sequencing.

These results suggest that the insert is present in the plasmid of the selected colonies. Moreover, we had to confirm if the insert had possitioned correctly and had the expected sequence so, plasmid DNA was sent for sequencing and the obtained sequence was compared to the *in silico* design.

2. Aggregative capacity of the CsgA-CRY-mCherry construct under light and dark conditions in E.coli.

The pRK2-CsgA-CRY-mCherry plasmid was designed to promote amyloid formation upon light exposure, due to the oligomerization properties of the cryptochrome domain. If the protein assembles correctly, the fusion protein is expected to adopt an amyloidogenic conformation capable of binding Congo Red, resulting in visibly red-stained bacterial colonies. **Figure 5** shows the behavior of different bacterial strains upon IPTG induction in Congo Red plates incubated at 25°C, a temperature known to optimize curli expression (Barnhart & Chapman, 2006). The assay was conducted under various conditions: bacterial cultures initiated either at an OD_{600} of 0.3 or from an overnight culture, and exposed either to light or dark environments. Notably, the *E.coli* BW25113 wild type – strain, which retains a functional curli operon, develops a distinct red coloration on the Congo Red medium independent if it is in dark or light conditions. This pigmentation is due to the expression of the curli protein which forms an extracellular amyloid structure that is capable of binding Congo Red. Interestingly, in

the *E. coli* strains lacking either CsgA or CsgB, grown in the dark, a more reddish coloration is observed in the center of the colony, surrounded by a peripheral white halo. A similar color pattern is also present in these two strains under light conditions, although the contrast between the center and the periphery is more subtle. In contrast, the bacteria's that contain the construct exhibit distinct behavior. Cultures initiated at an OD_{600} of 0.3 display noticeable slower growth compared to the BW25113 wild type and the Δ*csgA* and Δ*csgB* mutants. On the agar plates, this reduced growth is reflected by the presence of scattered, individual colonies rather than an uniform lawn. This observation suggests that, upon IPTG induction, the expressed construct may exert a toxic effect that impairs bacterial proliferation. Consequently, the sparse distribution of colonies complicates the assessment of Congo Red staining and makes color interpretation more challenging. Notably, in the Δ*csgB* strain harboring the plasmid grown in the dark, both red-colored colonies and white colonies can be observed, indicating heterogenous Congo Red binding. A similar color pattern is also present in the Δ*csgB* strain harboring the plasmid under light conditions. Nevertheless, when this strain is grown in the dark during the stationary phase, no Congo Red binding is observed, as evidence by the uniformly white appearance of the colonies. In contrast, when grown under light during the stationary phase, Congo Red binding becomes apparent, as indicated by a reddish coloration similar to that observed in the wild-type strain. This, in effect, indicates the aggregative capacity of the CsgA-CRY-mCherry plasmid and the capacity of oligomerization of the cryptochrome upon blue light exposure. The same color pattern can be observed in the Δ*CsgA* strain harboring the CsgA-CRY-mCherry plasmid.

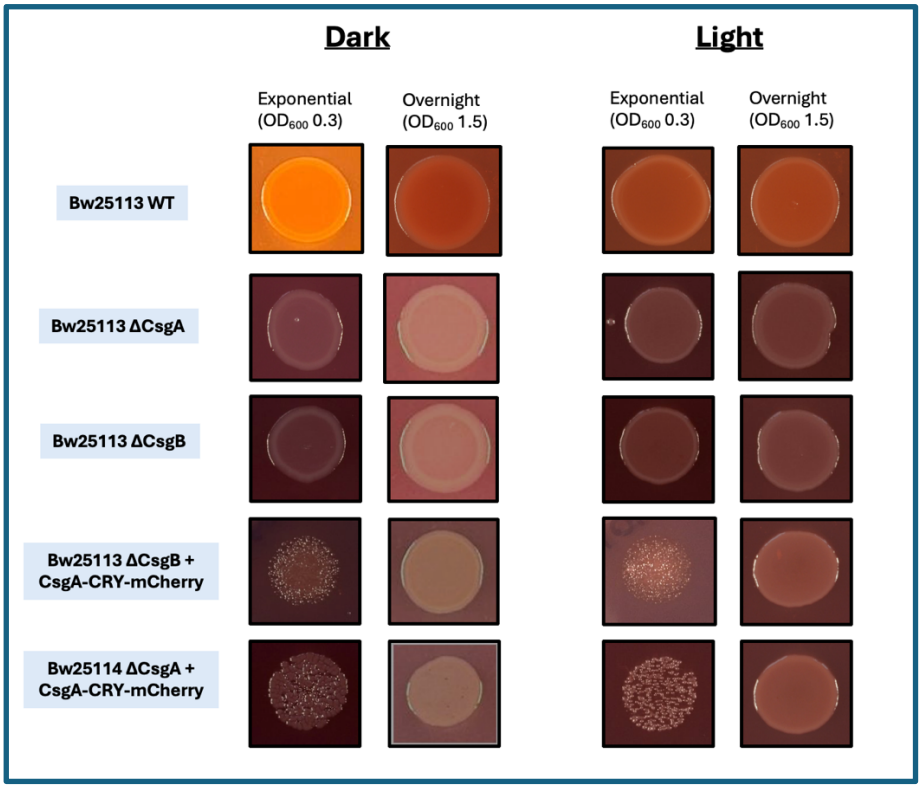

Figure 5. Aggregative capacity of CsgA-CRY-mCherry in Red Congo plates. Pannel A Dark conditions; pannel B: White light conditions.

3. Bacterial Protein expression assessed by Coomassie Blue staining and western blotting.

To assess the expression of the construct under IPTG induction, samples were collected at 0, 1 and 3 hours after induction. The culture was initiated at an OD_{600} of 0.05, and both Coomassie Blue staining and western blot analysis were performed in order to evaluate the protein expression over time. Aditionally, colony samples from the Congo Red plates were collected to detect the presence of the construct within the biofilm-associated cells.

The CsgA-CRY-mCherry has a molecular weight of ~100 kDa, therefore, a band at that weight should be expected to be seen in the Coomassie Blue stained gel and in the western blot. Nevertheless, too many and not defined bands are seen in both Coomasie stained gels (**Figure 6a) and 7a**). Moreover, it is difficult in **figure 7a)** to detect differential expression of native csgA (~15kDa) that should be seen in the BW25113 wt, Δ*csgB* and Δ*csgB* with CsgA-CRY-mCherry and the CsgA-CRY-mCherry (~100kDa) that should be seen in the Δ*csgA* and Δ*csgB* with the plasmid. Similarly, the western blot showed blurry, nonspecific signals, making it difficult to interpret the presence or absence of the fusion protein with confidence. In **figure**

6b), a faint signal appears around ~100 kDa in the 3-hour IPTG-induced sample. However, rather than a distinct band, the signal presents a smear, making it difficult for interpretation.

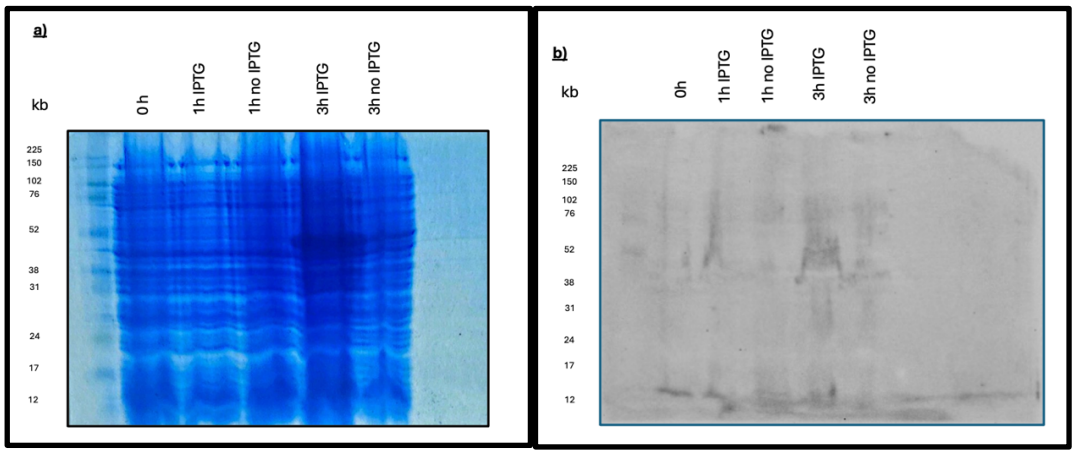

Figure 6. Coomassie Blue staning and western blotting of pRK2-CsgA-CRY-mCherry after IPTG induction in *E. coli* liquid cultures.

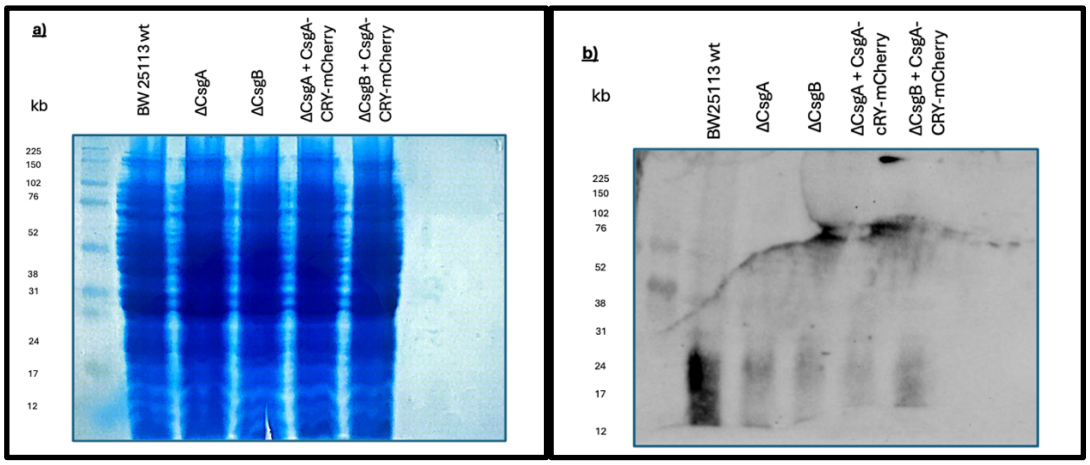

Figure 7. Coomassie Blue staining and western blotting of Congo Red Assay.

4. Detection of CsgA-CRY-mCherry in Δ*csgA E. coli* by fluorescence microscopy.

After IPTG induction in ΔcsgA pRK2-CsgA-CRY-mCherry *E.coli* samples were taken at T0 and T1h and visualized under fluoresence microscopy in order to see the presence of the plasmid. It can be seen that at T0h there is no red signal indicating no presence of the construct when there is no IPTG induction. At T1h there can be seen some red spots on the microscope indicating the presence of mCherry and thus, the CsgA-CRY-mCherry construct. This is shown by the black arrows in the pannel b of **figure 8**. Moreover, in this image it can also be seen some bacterial lisis indicating the toxicity of the construct (pink arrow).

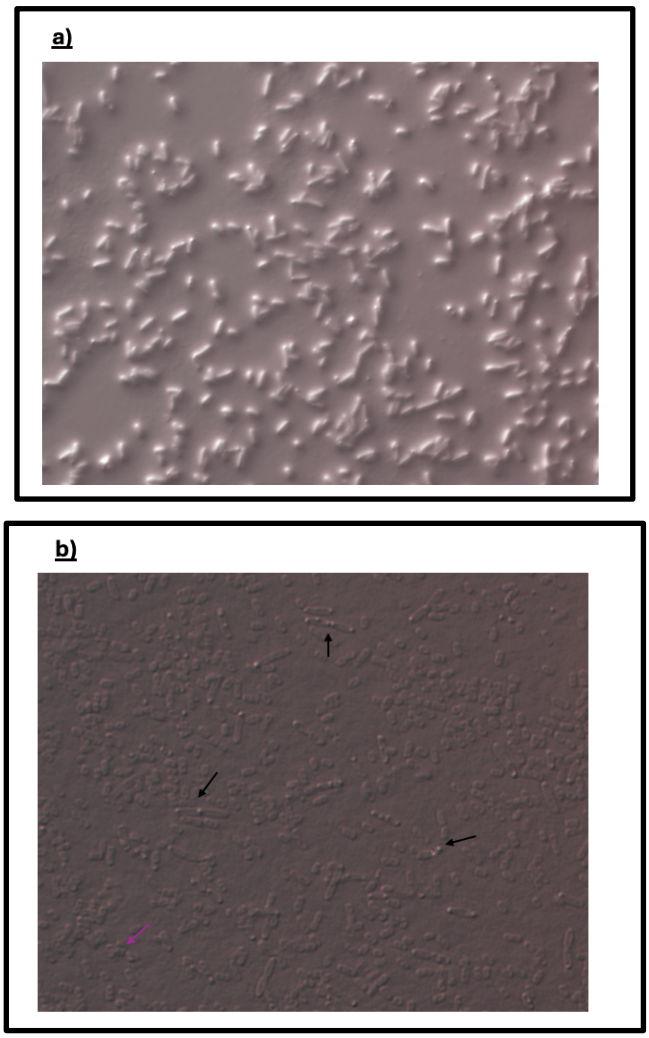

Figure 8. Fluoresence microscopy showing a) CsgA-CRY-mCherry in *E. coli* at T0h and b) T1h post IPTG induction. Black arrow showing red spots that indicate presence of CsgA-CRY-mCherry construct. Pink arrow highlights lysed bacteria.

5. *C. elegans* survival analysis to evaluate plasmid–induced neurotoxicity.

We performed a lifespan analysis under different conditions in order to evaluate plasmid induced neurotoxicity with Aß-CRY-mCherry transgenic *C. elegans*. This study compared the survival of transgenic *C. elgans* in comparison with *C. elegans* wild type (N2). The study began with 50 day 1 adult worm hermaphrodites and in figure 9 it can be seen that from day 2 to day 6, there is a more pronounced difference in survival comparing both conditions. It can be seen that at day 5, transgenic worms have ~40% survival vs. ~60% in N2. A t-test was performed in order to see if there is a statistical difference in the survival of the transgenic vs. non-transgenic for each time point. It can be seen that in the days 3, 7 amd 8 there is statistical difference shown by a $p<0.05$.

a)

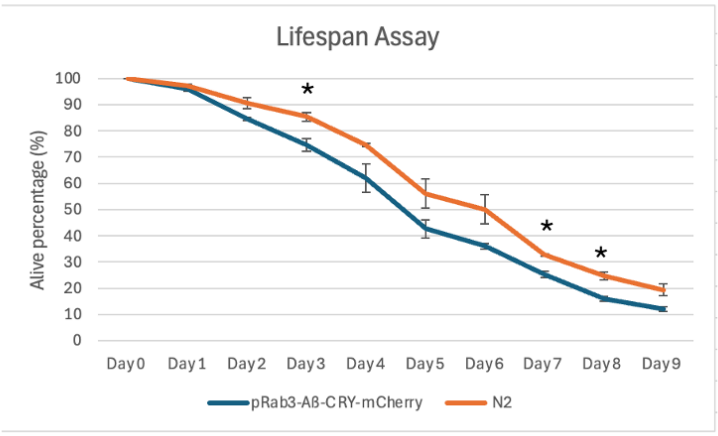

b)

	P value	Mean of Transgenic	Mean of Non - transgenic	Difference
		50.00	50.00	0.000
Day 1	0.373901	48.00	48.67	-0.6667
Day 2	0.073926	42.33	45.33	-3.000
Day 3	0.034920	37.33	42.67	-5.333
Day 4	0.108349	31.00	37.33	-6.333
Day 5	0.154273	21.33	28.00	-6.667
Day 6	0.098721	18.00	25.00	-7.000
Day 7	0.007933	12.67	16.33	-3.667
Day 8	0.014721	8.000	12.33	-4.333
Day 9	0.065109	6.000	9.667	-3.667

Figure 9. Lifespan assay for Aß-CRY-mCherry transgenic *C. elegans* and wild type (N2). A t-test was performed to compare the survival rates between transgenic and non-transgenic groups for each time points.

6. Detection and validation of expression of Aß-CRY-mCherry in *C.elegans* by western blot.

A whole worm lysate was performed in order to be able to detect the prab3-Aß-CRY-mCherry construct in *C. elegans* using a Anti-mCherry antibody. This construct has a molecular weight of ~96kda. A band of this weight can be identified in the whole worm lysate, yet, when performed the western blot, no signal was detected.

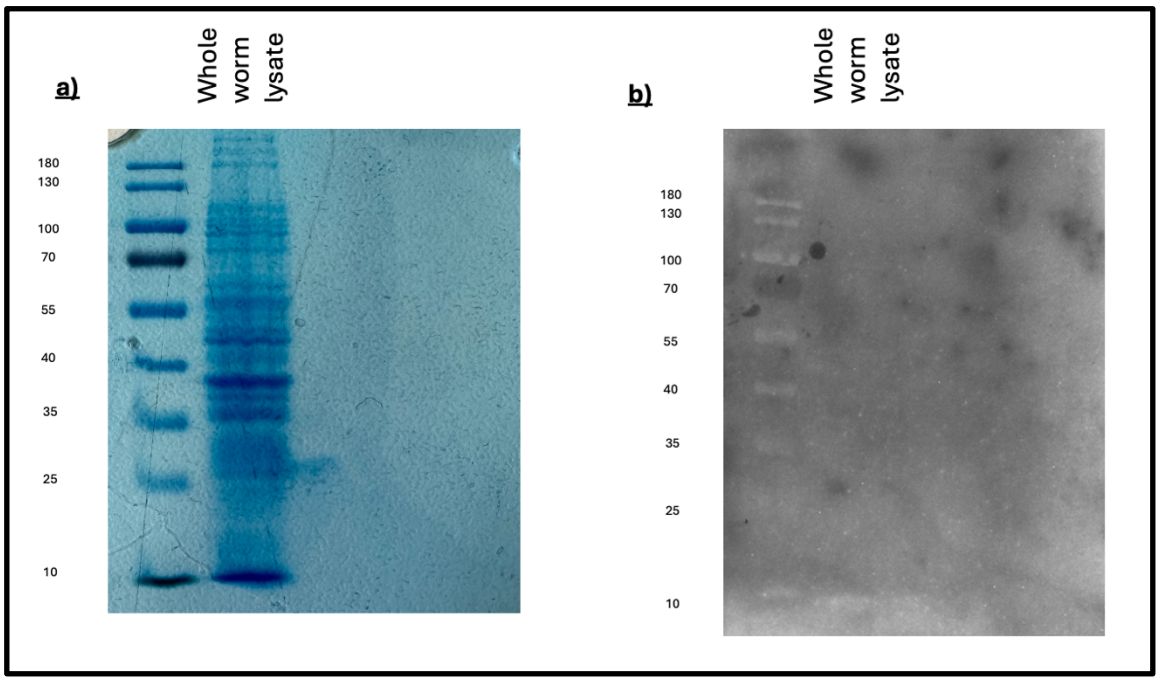

Figure 10. Coomassie Blue stain and western blot of whole worm lysate

Discussion

Characterizing the potential role of bacterial functional amyloids in the progression and severity of neurodegenerative diseases is a crucial step towards better understanding the disease mechanisms. This knowledge could potentially enable earlier interventions and ultimately lead to improved patient outcomes. That is why this project deeply aligns with the United Nations Sustainable Development Goals, particularly SDG3 (Good Health and Well-Being) by contributing to the knowledge pool of the molecular mechanisms underlying neurodegenerative diseases.

In this study, we aimed to develop and characterize a light-inducible amyloidogenic fusion protein, CsgA-CRY-mCherry, to explore the aggregation behaviour of bacterial amyloids in response to light stimulation. The intention of this fusion protein was to be posteriorly used so to be able to study *in vivo* the possible neurotoxic effects of the mayor subunit of curli (CsgA). Thus, the lifespan assay was intended to be conducted with CsgA-CRY-mCherry trasngenic *C. elegans* yet, time constrains did not allow for the generation of those transgenic animals within the project timeframe and so this assay was performed with Aß-CRY-mCherry transgenic *C. elegans* instead to gain experimental skills on this technique.

Prior characterization of the CsgA-CRY-mCherry fusion protein in bacterial systems is essential in order to validate its light-dependent aggregative behavior. This will make our

results in *C. elegans* reliable and confident that neurotoxicity can be attributed to amyloid formation. This step is fundamental in order to asses that the optogenetic tool works properly. The Congo Red assay indicates that the CsgA-CRY-mCherry construct undergoes amyloid oligomerization as WT CsgA under light conditions, as evidenced by the appearance of red-stained colonies both in the Δ*csgA* and Δ*csgB* strains harboring the plasmid. These red-stained colonies resemble those of the wild-type strain, although the coloration appears less intense. This suggest a lower degree of aggregation compared to the native curli system. Nevertheless, to confirm that the observed amyloid formation is specifically due to the fusion protein, it is essential to compare these results with the behavior of the same strains under dark conditions, as well as the untransformed Δ*csgA* and Δ*csgB* controls.

The production of this functional amyloid is necessary for biofilm formation and surface colonization (Brombacher et al., 2006; Cookson et al., 2002; Prigent-Combaret et al., 2001). The expression of this protein is associated with cellulose synthesis and contributes to the formation of the extracellular matrix, which plays a key role in mediating both cell-cell and cell-surface interactions. This is important to take into consideration because Congo Red can also bind to other cellular features such as cellulose (McCrate et al., 2013). Nevertheless, the BW25113 from the Keio collection is known to lack the ability to produce cellulose. Therefore, a positive Congo Red result in this strain would indicate the presence of curli fibers or a functional CsgA-CRY-mCherry fusion protein capable of forming amyloid structures (Nguyen et al., 2014; Sano et al., 2023).

In the Δ*csgA* and Δ*csgB* strains grown under dark conditions, the colonies exhibit a pinkish coloration with a surrounding white ring. This appearance differs from the deep red seen in the wild-type strains expressing functional curli, and therefore, the darker hue in the colony center cannot be conclusively attributed to amyloid formation. If there was indeed some residual protein expression (some part of the protein is being traduced), the appearance of the white halo and the non-uniform coloration might be explained by the fact that curli expression is enhacned under nutrient and oxygen-limited conditions, which are more pronounced at the center of the colony compared to the edges (Brombacher et al., 2006; Gerstel & Römling, 2001). Nevertheless, the behavior of the BW25113 Δ*csgA* mutant on Congo Red plates was already characterized in the laboratory and it showed a distinct white colony (negative for Congo Red). This is also seen for the BW25113 Δ*csgB* strain (Smith et al., 2017). Therefore, atrributing the red coloration observed to residual curli function in the Δ*csgA* or Δ*csgB* strain would be unlikely. Moreover, this mutants are generated by inserting a kanamycin resistance

cassette at the start codon and most of the coding sequence so not a functional protein can be translated (Baba et al., 2006). An alternative explanation for the presence of Congo Red in the Δ*csgA* and Δ*csgB* strains could be due to interbacterial complementation. It has been seen that when grown in proximity, a Δ*csgB* secretes soluble CsgA that can be assembled in the surface of a Δ*csgA*(Barnhart & Chapman, 2006). It could have happened that the proximity of the two strains on the same plate may have allowed aerosol-mediated transfer of secreted curli components. Although it is unlikely, this possibility should not be ruled out and in order to adress this, future assays should be done on separate plates. Under light conditions, the same strains exhibit a similarly pale pink coloration, although the tone appears slightly more uniform compared to the colonies grown in the dark. However, to draw definitive conclusions about the Congo Red phenotype of these strains, additional replicates are required.

In both Δ*csgA* and Δ*csgB* strains carrying the fusion protein, distinct individual colonies are observed when grown during the exponential phase. This may suggest that the construct is present and exerts a toxic effect on the bacteria, thereby reducing their growth rate. Regarding the Congo Red phenotype of these two strains under dark conditions, two distinct colony types are observed: some display a white or pale pinkish color while others appear more red. This is not the expected outcome under dark conditions for the Δ*csgB* harboring the construct as the cryptochrome is not anticipated to oligomerize in the absence of light (Park et al., 2017). Nevertheless, in the Δ*csgA* strain carrying the fusion protein (in both the exponential and stationary phase), a possible explanation for the possitive result seen could be a potential interaction between residual *csgB* in the strain and the plasmid-encoded *csgA*, which may allow for nucleation and subsequent aggregation. If this is the case, one possible explanation for the appearance of white colonies could be that the fusion protein is no longer functional. Although this seems unlikely given the presence of red colonies, it is possible that the construct´s toxicity leads to the silencing of the fusion protein for example by inserting a mobile genetic element such as a transposon or introducing a premature stop codon. To test this hypothesis, we will isolate both red and white colonies, grow them separetely on individual plates, and sequence them to determine whether the protein fusion remains intact. Nevertheless, because of this, a double mutant Δ*csgA*/Δ*csgB* was planned in order to eliminate this possibility. Interestingly, when the Δ*csgB* strain harboring the plasmid is grown during the stationary phase, the resulting colonies appear white, suggesting the absence of amyloid fiber formation. One possible explanation for the contrasting phenotype observed in exponential phase cultures could be due to contamination with curli-producing wild-type *E. coli.* Moreover, it can be seen that in the

Δ*csgA* strain harboring the plasmid when grown during the exponential phase in dark conditions a intense pink color is observed, yet, this red color is distinct from the Congo Red staining seen in wild-type strains, and may instead be attributed to localized pigment retention rather than true amyloid deposition. In this strain it also occurs that when grown in an OD_{600} nm of 0.03 it shows a red color and when grown with an overnight color it appears white.

The detection of apparent curli expression when grown in the exponential phase but not in stationary phase is unexpected. As curli fimbriae are generally expressed during the transition to stationary phase at temperatures below 30 °C (Pesavento et al., 2008). Therefore, it is strange to observe white colonies in the strains derived from an overnight culture, while those grown from the exponential phase cultures (OD_{600} nm 0.3) display red coloration. We would expect stronger Congo Red binding in the overnight cultures as they have spent more time in the stationary phase. The appearance of white colonies from overnight cultures and red ones from exponential-phase cultures is, therefore, puzzling. This further supports the possibility that the phenotype observed in exponential phase cultures may result from contamination, and thus the experiment should be repeated.

Regarding the Congo Red phenotype of the Δ*csgA* and Δ*csgB* harboring the construct under light conditions, red coloration was observed in both the OD_{6oo} nm of 0.3 and overnight. This is indicative of amyloid formation and Congo Red binding. However, given that the results under dark conditions remain inconclusive, further repetitions of the experiment are required to confirm whether the fusion protein is correctly assembling into amyloid structure.

Furthermore, it should have been taken in consideration the fact that the cryptochrome from *Arabidopsis thaliana* needs FADas a cofactor for light-induced activation(Palayam et al., 2021). While this does not suppose a problem for the assay in *C. elegans* -where the protein is not secreted- it may represent a critical factor in the Congo Red binding essay, as the fusion protein is secreted to the extracelular medium. In this context, it might occur that the cryptochrome won´t oligomerize properly due to the absence of FAD. To address this, the bacteria could be cultured in a medium supplemented with FAD to ensure the availability of the cofactor during the assay.

Additionally, optimization of the procedure for the Congo Red plates is recommended. One variable to consider is the dye concentration: while our protocol used 50 µg/mL of Congo Red, a study by Reichhardt et al. (2015) examining the interaction between Congo Red an curli-producing *E. coli* utilized lower concentration of 25 µg/mL (Reichhardt et al., 2015). This

higher concentration in our experiment may have contributed to nonspecific binding, potentially explaining the red coloration observed under conditions where curli expression is not expected. Moreover, since 1L of Congo Red agar was prepared in bulk and then poured into individual plates, it is possible that the antibiotic was not evenly distributed across all plates or even within each plate, potentially leading to the loss of the resistance cassete and the restoration of the *csgA* or *csgB* expression. This could lead to confusing results in the Congo Red phenotyping.

To accurately determine what is being produced in the Congo Red assay, the Western blot was intended as a complementary method. An expected band of ~100 kda should have been present in the Δ*csgA* and Δ*csgB* harboring the construct. Moreover, the antibody should also recognize the native *csgA*, thus, we would have expected a band in the E. coli BW25113 wild-type, in the Δ*csgB* and in the Δ*csgB* harboring the construct. Thus, if a signal is detected in the Δ*csgA* colonies using anti-CsgA antibody, this would indicate possible contamination. Nevertheless, the absence of a band around ~100 kDa in the Δ*csgA* and Δ*csgB* strains harboring the construct does not suggest entirely the absence of the fusion protein. This may reflect the need to optimize experimental conditions and should also consider that amyloid fibers are resistant to SDS, potentially afecting their detection.

Nevertheless, both the Coomassie Blue staining gel and the western blot failed to provide useful or conclusive information. However, these techniques remain valuable tools for evaluating our protein fusion, provided that the experimental protocol is properly optimized. As a first step, we performed both a Coomassie-blue stained SDS-PAGE and western blot using samples adjusted to an OD_{600} nm of 0.2, loading 15 µL of lysate per well. However, under these conditions, we observed little to no visible bands in the Coomasie blue stained gel and no detectable signal in the western blot. For this reason, we decided to carry out a second induction assay, in which we collected bacterial cultures at an OD_{600} nm of 1.0 and subsequently loaded 25 µL of each lysate sample into the gel. Yet, the result was an excessive protein concentration that led to poorly defined bands and extensive smearing. This issue could have been mitigating by loading only the soluble protein fraction onto the SDS-PAGE gel. This would involve performing cell lysis, centrifuging the samples to remove cellular debris, and subsequently quantifying the protein concentration using Bradford Assay in order to load equal amounts of total protein in each well which would have ensured better comparability between the samples. Moreover, avoiding gel overloading would have resulted in better-defined bands, promoting

more even antibody binding and reducing the non-specific interactions. This would have improved the overall signal clarity and removed background noise in the western blot.

Fluorescence microscopy was used as an additional method to assess protein expression in Δ*csgA E. coli* following IPTG induction. This technique allows the detection of mCherry fluorescence under green excitation light, serving as an indicator of protein expression. As shown in **Figure 8**, without IPTG induction, no fluorescence signfal is observed, conssitent with the repression of the expression by the pTac promoter. On the other hand, at 1 hour post-induction, discrete red spots are visible likely on the bacteria indicating successful expression and aggregation of the CsgA-CRY-mCherry plasmid. Nevertheless, there are very few spots indicating low expression. In the **figure 8 pannel b** some blury spots can be seen, which indicate bacterial lysis (shown by the pink arrow). This indicates that the construct may impose toxicity to the bacteria and thus, this indicates that the construct is efectively being expressed. Moreover, on the Congo Red assay it can be seen that the strains harboring the plasmid had a slower growth than the ones without the plasmid indicating that the protein fusion may impose a metabolic burden. It has been seen that bacteria can reduce the plasmid copy number if this imposes toxicity to the bacteria (Ruan & Bourne, 2024). This could explain the low levels of functional fusion protein. Therefore, the observed low protein expression can be due to bacterial survival mechanism in response to the potential toxicity of the construct. However, it may also result from low IPTG concentration (0.05mM). Repeating the experiment with higher IPTG concentration could help clarify whether the limited expression is due to the bacterial adaptation to a toxic protein or insufficient induction.

The lifespan analysis of the Aß-CRY-mCherry transgenic *C. elegans* showed a difference in the survival in comparison to the non-transgenic *C. elegans*. In **figure 9 pannel a)** shows that from day 3 to day 5, the transgenic nematodes died faster than the non transgenic. Yet, the overall survival was not significantly different given the fact that at day 9 (last day of the study) there was no significant difference in the survival of the transgenic vs. non transgenic nematodes. When analyzing these results, what can be concluded is that the construct accelerates aging but not the overall lifespan of the nematode. Nevertheless, the lifespan assay should have been performed until the day where 0 nematodes were left, yet, due to time constraints it had to be stopped at day 9.

When we attempted to detect the fusion protein by western blotting using whole nematode lysates, no signal was observed. We went steps backwards and discovered that the

construct contained a premature stop codon caused by an extra nucleotide at the end of the Aß peptide sequence, which likely prevented proper translation of the full fusion protein. The toxicity observed in the survival analysis of transgenic vs. non-transgenic nematodes can no longer be attributed to the oligomerization of the fusion protein but rather to the Aß peptide *per se*. This explains what we observed in another survival analysis that was started but not finished in which we saw no difference in the survival rate of the Aß-CRY-mCherry transgenic nematodes exposed to light vs. the transgenic nematodes grown in the dark. The absence of cryptochrome in this case prevents light-dependent oligomerization, and therefore, a decrease in survival in the light exposed transgenic nematodes is not expected.

Conclusion

In this study we were able to design and partially characterize an optogenetic fusion protein (CsgA-CRY-mCherry) to investigate the potential neurotoxic effects of CsgA, the major subunit of the curli protein using as an animal model *Caenorhabditis elegans*. This optogenetic tools allows for spatiotemporal control over the bacterial amyloid aggregation.

Our results suggest that the construct is able of aggregating under light conditions, as evidenced by positive result in the Congo Red assay observed in the Δ*csgA* and Δ*csgB* mutants expressing the fusion protein. Nevertheless, these results are inconclusive due to the appearance of red in the dark conditions grown in the exponential phase and absence of clearly defined bands both in the SDS-PAGE and western blot analysis. These issues indicate a need of protocol optimization and experiment repetition in order to have clear and confident results.

In parallel, the use of Aß-CRY-mCherry transgenic *C. elegans* as a control showed an earlier increase in mortality, yet, due to the discovery of a premature codon stop in this construct it invalidates its use for evaluating the effect of blue light oligomerization. This indicates that the toxicity is not due to oligomerization but because of the Aß peptide alone.

Despite the limitations, this project demonstrates a promising use of optogenetics to study the potential neurotoxicity of bacterial amyloids in vivo and its potential relation with the severity and progression of neurodegenerative diseases.

Bibliography

Baba, T., Ara, T., Hasegawa, M., Takai, Y., Okumura, Y., Baba, M., Datsenko, K. A., Tomita, M., Wanner, B. L., & Mori, H. (2006). Construction of Escherichia coli K-12 in-frame, single-gene knockout mutants: the Keio collection. *Molecular Systems Biology*, *2*, 2006.0008. https://doi.org/10.1038/MSB4100050

Barnhart, M. M., & Chapman, M. R. (2006). Curli biogenesis and function. *Annual Review of Microbiology*, *60*, 131–147. https://doi.org/10.1146/ANNUREV.MICRO.60.080805.142106,

Berer, K., Mues, M., Koutrolos, M., AlRasbi, Z., Boziki, M., Johner, C., Wekerle, H., & Krishnamoorthy, G. (2011). Commensal microbiota and myelin autoantigen cooperate to trigger autoimmune demyelination. *Nature*, *479*(7374), 538–541. https://doi.org/10.1038/NATURE10554,

Brombacher, E., Baratto, A., Dorel, C., & Landini, P. (2006). Gene expression regulation by the curli activator CsgD protein: Modulation of cellulose biosynthesis and control of negative determinants for microbial adhesion. *Journal of Bacteriology*, *188*(6), 2027–2037. https://doi.org/10.1128/JB.188.6.2027-2037.2006,

Chapman, M. R., Robinson, L. S., Pinkner, J. S., Roth, R., Heuser, J., Hammar, M., Normark, S., & Hultgren, S. J. (2002). Role of Escherichia coli Curli Operons in Directing Amyloid Fiber Formation. *Science (New York, N.Y.)*, *295*(5556), 851. https://doi.org/10.1126/SCIENCE.1067484

Chen, S. G., Stribinskis, V., Rane, M. J., Demuth, D. R., Gozal, E., Roberts, A. M., Jagadapillai, R., Liu, R., Choe, K., Shivakumar, B., Son, F., Jin, S., Kerber, R., Adame, A., Masliah, E., & Friedland, R. P. (2016). Exposure to the Functional Bacterial Amyloid Protein Curli Enhances Alpha-Synuclein Aggregation in Aged Fischer 344 Rats and Caenorhabditis elegans. *Scientific Reports*, *6*. https://doi.org/10.1038/srep34477

Cherny, I., Rockah, L., Levy-Nissenbaum, O., Gophna, U., Ron, E. Z., & Gazit, E. (2005). The formation of Escherichia coli curli amyloid fibrils is mediated by prion-like peptide repeats. *Journal of Molecular Biology*, *352*(2), 245–252. https://doi.org/10.1016/J.JMB.2005.07.028

Cook, S. J., Jarrell, T. A., Brittin, C. A., Wang, Y., Bloniarz, A. E., Yakovlev, M. A., Nguyen, K. C. Q., Tang, L. T. H., Bayer, E. A., Duerr, J. S., Bülow, H. E., Hobert, O., Hall, D. H., & Emmons, S. W. (2019). Whole-animal connectomes of both Caenorhabditis elegans sexes. *Nature 2019 571:7763*, *571*(7763), 63–71. https://doi.org/10.1038/s41586-019-1352-7

Cookson, A. L., Cooley, W. A., & Woodward, M. J. (2002). The role of type 1 and curli fimbriae of Shiga toxin-producing Escherichia coli in adherence to abiotic surfaces. *International Journal of Medical Microbiology*, *292*(3–4), 195–205. https://doi.org/10.1078/1438-4221-00203

Cryan, J. F., O'Riordan, K. J., Sandhu, K., Peterson, V., & Dinan, T. G. (2020). The gut microbiome in neurological disorders. *The Lancet. Neurology*, *19*(2), 179–194. https://doi.org/10.1016/S1474-4422(19)30356-4

Evans, M. L., Chorell, E., Taylor, J. D., Åden, J., Götheson, A., Li, F., Koch, M., Sefer, L., Matthews, S. J., Wittung-Stafshede, P., Almqvist, F., & Chapman, M. R. (2015). The bacterial curli system possesses a potent and selective inhibitor of amyloid formation. *Molecular Cell*, *57*(3), 445–455. https://doi.org/10.1016/j.molcel.2014.12.025

Frid, P., Anisimov, S. V., & Popovic, N. (2007). Congo red and protein aggregation in neurodegenerative diseases. *Brain Research Reviews*, *53*(1), 135–160. https://doi.org/10.1016/j.brainresrev.2006.08.001

Friedland, R. P., & Chapman, M. R. (2017). The role of microbial amyloid in neurodegeneration. *PLoS Pathogens*, *13*(12). https://doi.org/10.1371/JOURNAL.PPAT.1006654

Friedland, R. P., McMillan, J. D., & Kurlawala, Z. (2020). What are the molecular mechanisms by which functional bacterial amyloids influence amyloid beta deposition and neuroinflammation in neurodegenerative disorders? In *International Journal of Molecular Sciences* (Vol. 21, Issue 5). MDPI AG. https://doi.org/10.3390/ijms21051652

Fujii, Y., Nguyen, T. T. T., Fujimura, Y., Kameya, N., Nakamura, S., Arakawa, K., & Morita, H. (2019). Fecal metabolite of a gnotobiotic mouse transplanted with gut microbiota from a patient with Alzheimer's disease. *Bioscience, Biotechnology and Biochemistry*, *83*(11), 2144–2152. https://doi.org/10.1080/09168451.2019.1644149,

Gallo, P. M., Rapsinski, G. J., Wilson, R. P., Oppong, G. O., Sriram, U., Goulian, M., Buttaro, B., Caricchio, R., Gallucci, S., & Tükel, Ç. (2015). Amyloid-DNA Composites of Bacterial Biofilms Stimulate Autoimmunity. *Immunity*, *42*(6), 1171–1184. https://doi.org/10.1016/j.immuni.2015.06.002

Gerstel, U., & Römling, U. (2001). Oxygen tension and nutrient starvation are major signals that regulate agfD promoter activity and expression of the multicellular morphotype in Salmonella typhimurium. *Environmental Microbiology*, *3*(10), 638–648. https://doi.org/10.1046/J.1462-2920.2001.00235.X;WGROUP:STRING:PUBLICATION

Hammar, M., Arnqvist, A., Bian, Z., Olsén, A., & Normark, S. (1995). Expression of two csg operons is required for production of fibronectin- and Congo red-binding curli polymers in Escherichia coli K-12. *Molecular Microbiology*, *18*(4), 661–670. https://doi.org/10.1111/J.1365-2958.1995.MMI_18040661.X

Hsien, L. C., Kaur, P., Teo, E., Lam, V. Y. M., Zhu, F., Kibat, C., Gruber, J., Mathuru, A., & Tolwinski, N. S. (2020). Application of optogenetic amyloid-β distinguishes between metabolic and physical damage in neurodegeneration. *ELife*, *9*. https://doi.org/10.7554/ELIFE.52589

Intili, G., Paladino, L., Rappa, F., Alberti, G., Plicato, A., Calabrò, F., Fucarino, A., Cappello, F., Bucchieri, F., Tomasello, G., Carini, F., & Pitruzzella, A. (2023). From Dysbiosis to Neurodegenerative Diseases through Different Communication Pathways: An Overview. *Biology 2023, Vol. 12, Page 195*, *12*(2), 195. https://doi.org/10.3390/BIOLOGY12020195

Kim, W., Underwood, R. S., Greenwald, I., & Shaye, D. D. (2018). OrthoList 2: A New Comparative Genomic Analysis of Human and Caenorhabditis elegans Genes. *Genetics*, *210*(2), 445–461. https://doi.org/10.1534/GENETICS.118.301307

Loh, J. S., Mak, W. Q., Tan, L. K. S., Ng, C. X., Chan, H. H., Yeow, S. H., Foo, J. B., Ong, Y. S., How, C. W., & Khaw, K. Y. (2024). Microbiota–gut–brain axis and its therapeutic applications in neurodegenerative diseases. *Signal Transduction and Targeted Therapy 2024 9:1*, *9*(1), 1–53. https://doi.org/10.1038/s41392-024-01743-1

McCrate, O. A., Zhou, X., & Cegelski, L. (2013). Curcumin as an Amyloid-indicator Dye in E. coli. *Chemical Communications (Cambridge, England)*, *49*(39), 4193. https://doi.org/10.1039/C2CC37792F

Molina-García, L., Moreno-del Álamo, M., Botias, P., Martín-Moldes, Z., Fernández, M., Sánchez-Gorostiaga, A., Alonso-del Valle, A., Nogales, J., García-Cantalejo, J., & Giraldo, R. (2017). Outlining core pathways of amyloid toxicity in bacteria with the RepA-WH1 prionoid. *Frontiers in Microbiology*, *8*(APR). https://doi.org/10.3389/FMICB.2017.00539,

Nenninger, A. A., Robinson, L. S., & Hultgren, S. J. (2009). Localized and efficient curli nucleation requires the chaperone-like amyloid assembly protein CsgF. *Proceedings of the National Academy of Sciences of the United States of America*, *106*(3), 900. https://doi.org/10.1073/PNAS.0812143106

Nguyen, M. H., Ojima, Y., Sakka, M., Sakka, K., & Taya, M. (2014). Probing of exopolysaccharides with green fluorescence protein-labeled carbohydrate-binding module in Escherichia coli biofilms and flocs induced by bcsB overexpression. *Journal of Bioscience and Bioengineering*, *118*(4), 400–405. https://doi.org/10.1016/J.JBIOSC.2014.03.005

O'Nuallain, B., Williams, A. D., Westermark, P., & Wetzel, R. (2004). Seeding specificity in amyloid growth induced by heterologous fibrils. *The Journal of Biological Chemistry*, *279*(17), 17490–17499. https://doi.org/10.1074/JBC.M311300200

Orobets, K. S., & Karamyshev, A. L. (2023). Amyloid Precursor Protein and Alzheimer's Disease. *International Journal of Molecular Sciences*, *24*(19). https://doi.org/10.3390/IJMS241914794,

Palayam, M., Ganapathy, J., Guercio, A. M., Tal, L., Deck, S. L., & Shabek, N. (2021). Structural insights into photoactivation of plant Cryptochrome-2. *Communications Biology*, *4*(1), 1–11. https://doi.org/10.1038/S42003-020-01531-X;TECHMETA=101,82,9;SUBJMETA=1266,2686,449,45,535,631;KWRD=LIGHT+RESPONSES,STRUCTURAL+BIOLOGY,X-RAY+CRYSTALLOGRAPHY

Park, H., Kim, N. Y., Lee, S., Kim, N., Kim, J., & Heo, W. Do. (2017). Optogenetic protein clustering through fluorescent protein tagging and extension of CRY2 /631/80/86 /631/1647/2253 /631/61/338/552 article. *Nature Communications*, *8*(1), 1–8. https://doi.org/10.1038/S41467-017-00060-2;SUBJMETA=1647,2253,338,552,61,631,80,86;KWRD=CELL+SIGNALLING,OPTOGENETICS,SYNTHETIC+BIOLOGY

Perov, S., Lidor, O., Salinas, N., Golan, N., Tayeb-Fligelman, E., Deshmukh, M., Willbold, D., & Landau, M. (2019). Structural Insights into Curli CsgA Cross-β Fibril Architecture Inspire Repurposing of Anti-amyloid Compounds as Anti-biofilm Agents. *PLoS Pathogens*, *15*(8). https://doi.org/10.1371/JOURNAL.PPAT.1007978

Pesavento, C., Becker, G., Sommerfeldt, N., Possling, A., Tschowri, N., Mehlis, A., & Hengge, R. (2008). Inverse regulatory coordination of motility and curli-mediated adhesion in Escherichia coli. *Genes & Development*, *22*(17), 2434–2446. https://doi.org/10.1101/GAD.475808

Prigent-Combaret, C., Brombacher, E., Vidal, O., Ambert, A., Lejeune, P., Landini, P., & Dorel, C. (2001). Complex regulatory network controls initial adhesion and biofilm formation in Escherichia coli via regulation of the csgD gene. *Journal of Bacteriology*, *183*(24), 7213–7223. https://doi.org/10.1128/JB.183.24.7213-7223.2001,

Reichhardt, C., Jacobson, A. N., Maher, M. C., Uang, J., McCrate, O. A., Eckart, M., & Cegelski, L. (2015). Congo red interactions with curli-producing E. coli and native curli amyloid fibers. *PLoS ONE*, *10*(10). https://doi.org/10.1371/JOURNAL.PONE.0140388,

Robinson, L. S., Ashman, E. M., Hultgren, S. J., & Chapman, M. R. (2006). Secretion of curli fibre subunits is mediated by the outer membrane-localized CsgG protein. *Molecular Microbiology*, *59*(3), 870–881. https://doi.org/10.1111/J.1365-2958.2005.04997.X,

Ruan, S., & Bourne, C. R. (2024). Escherichia coli cells evade inducible parE toxin expression by reducing plasmid copy number . *Microbiology Spectrum*, *12*(6). https://doi.org/10.1128/SPECTRUM.03973-23,

Sano, K., Kobayashi, H., Chuta, H., Matsuyoshi, N., Kato, Y., & Ogasawara, H. (2023). CsgI (YccT) Is a Novel Inhibitor of Curli Fimbriae Formation in Escherichia coli Preventing CsgA Polymerization and Curli Gene Expression. *International Journal of Molecular Sciences*, *24*(5). https://doi.org/10.3390/IJMS24054357,

Smith, D. R., Price, J. E., Burby, P. E., Blanco, L. P., Chamberlain, J., & Chapman, M. R. (2017). The production of curli amyloid fibers is deeply integrated into the biology of escherichia coli. *Biomolecules*, *7*(4). https://doi.org/10.3390/BIOM7040075,

Taylor, J. D., & Matthews, S. J. (2015). New insight into the molecular control of bacterial functional amyloids. *Frontiers in Cellular and Infection Microbiology*, *5*(APR). https://doi.org/10.3389/FCIMB.2015.00033,

Torres, A. K., Mira, R. G., Pinto, C., & Inestrosa, N. C. (2025). Studying the mechanisms of neurodegeneration: C. elegans advantages and opportunities. *Frontiers in Cellular Neuroscience*, *19*, 1559151. https://doi.org/10.3389/FNCEL.2025.1559151/XML/NLM

Tursi, S. A., & Tükel, Ç. (2018). Curli-Containing Enteric Biofilms Inside and Out: Matrix Composition, Immune Recognition, and Disease Implications. *Microbiology and Molecular Biology Reviews*, *82*(4). https://doi.org/10.1128/MMBR.00028-18,

Unger, M. M., Spiegel, J., Dillmann, K. U., Grundmann, D., Philippeit, H., Bürmann, J., Faßbender, K., Schwiertz, A., & Schäfer, K. H. (2016). Short chain fatty acids and gut microbiota differ between patients with Parkinson's disease and age-matched controls. *Parkinsonism & Related Disorders*, *32*, 66–72. https://doi.org/10.1016/J.PARKRELDIS.2016.08.019

Wang, C., Lau, C. Y., Ma, F., & Zheng, C. (2021). Genome-wide screen identifies curli amyloid fibril as a bacterial component promoting host neurodegeneration. *Proceedings of the National Academy of Sciences of the United States of America*, *118*(34). https://doi.org/10.1073/PNAS.2106504118/-/DCSUPPLEMENTAL

Wang, X., & Chapman, M. R. (2008). Sequence Determinants of Bacterial Amyloid Formation. *Journal of Molecular Biology*, *380*(3), 570–580. https://doi.org/10.1016/J.JMB.2008.05.019

Wang, X., Hammer, N. D., & Chapman, M. R. (2008). The molecular basis of functional bacterial amyloid polymerization and nucleation. *The Journal of Biological Chemistry*, *283*(31), 21530–21539. https://doi.org/10.1074/JBC.M800466200

Zheng, P., Zeng, B., Liu, M., Chen, J., Pan, J., Han, Y., Liu, Y., Cheng, K., Zhou, C., Wang, H., Zhou, X., Gui, S., Perry, S. W., Wong, M. L., Licinio, J., Wei, H., & Xie, P. (2019). The gut microbiome from patients with schizophrenia modulates the glutamate-glutamine-GABA cycle and schizophrenia-relevant behaviors in mice. *Science Advances*, *5*(2). https://doi.org/10.1126/SCIADV.AAU8317,

Appendix

1. Primers

Name	Sequence	Function
Rab3-Aß vector_Fwd	gtacaagtagGAGCTCCGCATCGGCCGC	Forward primer used for the amplification of the vector backbone for pRab3-Aß-CRY-mCherry from pRab3-Aß-NV1
Rab3-Aß vector_Rev	ccatcttcatCTCGAGTAGCAATGACAACTCC TCCCAC	Reverse primer used for the amplification of the vector backbone for pRab3-Aß-CRY-mCherry from pRab3-Aß-NV1
CRY-mCherry inser_Fwd	gctactcgagATGAAGATGGACAAAAAGAC	Forward primer used for the amplification of the insert for pRab3-Aß-CRY-mCherry from pDONOR-CRY-mCherry
CRY-mCherry inser_Rev	tgcggagctcCTACTTGTACAGCTCGTC	Reverse primer used for the amplification of the insert for pRab3-Aß-CRY-mCherry from pDONOR-CRY-mCherry
Rab3-CRY-mCherry vector_Fwd	ttcatccggaATGAAGATGGACAAAAAGAC	Forward primer used for the amplification of the vector backbone for pRab3-CsgA-CRY-mCherry from pRab3-Aß-CRY-mCherry
Rab3-CRY-mCherry vector_Rev	ccggggatccCTGAAAATAGGGCTACTG	Reverse primer used for the amplification of the vector backbone for

		pRab3-CsgA-CRY-mCherry from pRab3-Aß-CRY-mCherry
CsgA inser_Fwd	ctattttcagGGATCCCCGGGATTGGCC	Forward primer used for the amplification of the insert pRab3-CsgA-RFP
CsgA inser_Rev	ccatcttcatTCCGGATGAACCAGAGCTTCC	Reverse primer used for the amplification of the insert pRab3-CsgA-RFP
Vector prk2 CsgA_fwd	TGAAGCTTGCATGCCTGC	Forward primer used for the amplification of the vector backbone for pRK2-CsgA-CRY-mCherry from pRK2-CsgA-NV1
Vector prk2 CsgA_rev	GTACTGATGAGCGGTCGC	Reverse primer used for the amplification of the vector backbone for pRK2-CsgA-CRY-mCherry from pRK2-CsgA-NV1
link-CRY-mCherry inser_fwd	acgcgaccgctcatcagtac GGAAGCTCTGGTTCATCC	Forward primer used for the amplification of the insert for pRK2-CsgA-CRY-mCherry
link-CRY-mCherry inser_rev	ctgcaggcatgcaagcttcaCTACTTGTACAGCTC GTC	Reverse primer used for the amplification of the insert for pRK2-CsgA-CRY-mCherry

Table 1 Appendix: Primers used for PCR amplification and sequencing.

2. *C. elegans* strains

Name	Genotype	Precedence
MOP2	momEx2[pLRH-1(rab-3::Ab::CRY::mCHerry(20ng/µL); cc::GFP (30ng/µL)	This study
N2	*C. elegans* Bristol isolate	CGC

Table 2 Appendix. *C. elegans* strains used.

3. Bacterial strains

Name	Precedence
DH5α	New England Biolabs
BW25113	Keio Collection
BW25113 Δ*csgA*	Keio Collection
BW25113 Δ*csgB*	Keio Collection
BW25113 Δ*csgA*+ pRK2-CsgA-CRY-mCherry	This study
BW25113 Δ*csgB* + pRK2-CsgA-CRY-mCherry	This study

Table 3 Appendix. Bacterial strains used.